DOI: 10.7641/CTA.2013.12126

三电机驱动系统的神经网络模糊自整定解耦控制

张　浩[1,2†], 于　堃[2], 刘国海[2], 胡德水[2], 赵文祥[2]

(1. 东南大学 复杂工程系统测量与控制教育部重点实验室, 江苏 南京 210096; 2. 江苏大学 电气信息工程学院, 江苏 镇江 212013)

摘要: 多电机驱动系统是一种多输入多输出、非线性、强耦合的系统. 它广泛应用在许多需要高精度协调控制的驱动领域, 比如电动汽车驱动、城市轨道交通以及印刷业等. 本文提出了一种新的方法用于三电机驱动系统的速度与张力的解耦控制, 其核心由模糊自整定控制与BP神经网络广义逆组成. 首先, 由神经网络广义逆与原系统串联实现复合伪线性系统; 其次, 在该伪线性系统中采用模糊自整定方法. 仿真结果表明: 所提方法能有效实现速度与张力间的解耦, 将三电机驱动系统转化为多个具有开环稳定性的单输入单输出线性子系统, 同时系统的响应速度快、超调量小、瞬态时间较短, 具有良好的跟踪性能, 这有助于改善系统的启动特性, 降低系统振荡.

关键词: 三电机驱动; 模糊自整定控制; 启动特性; 神经网络广义逆

中图分类号: TP273　　**文献标识码**: A

Fuzzy self-tuning decoupling control based on neural network of three-motor drive system

ZHANG Hao[1,2†], YU Kun[2], LIU Guo-hai[2], HU De-shui[2], ZHAO Wen-xiang[2]

(1. Key Laboratory of Measurement and Control of Complex System of Engineering of Ministry of Education, Southeast University, Nanjing Jiangsu 210096, China;
2. School of Electrical and Information Engineering, Jiangsu University, Zhenjiang Jiangsu 212013, China)

Abstract: Multi-motor drive system is a multi-input multi-output (MIMO), nonlinear and strong-coupling system. It is applied to many drive fields where high precision coordinated control is of importance, such as the electric vehicle drive, urban rail transit, and printing. In this paper, a new control strategy is proposed for decoupling the speed and the tension of the three-motor drive system, in which the key is to incorporate the fuzzy self-tuning control with back-propagation (BP) neural network generalized inverse (NNGI). The pseudo-linear composite system is formed by connecting NNGI in series with the original system; and then, the fuzzy self-tuning control method is introduced to this pseudo-linear system. Simulation results demonstrate that the proposed strategy can effectively decouple speeds and tensions, and transform the three-motor drive system into several single-input single-output (SISO) linear subsystems with open-loop stability. This system has obvious superiority in rapid response speed, low overshoot, short transient time and good tracking effect, which help to improve the starting characteristics of the system and decrease the system oscillation.

Key words: three-motor drive; fuzzy self-tuning control; starting characteristics; neural network generalized inverse

1 Introduction

High precision coordinated control performance is an essential requirement for industrial drive applications, where any kind of mistakes may lead to the fault of the assembly line.

In recent years, theoretical and experimental studies on multi-motor drive system have seen fast development. Sustainable and high efficient operation of motor drives has been a growing focus, especially for the electric vehicle drive, urban rail transit, printing, and so on[1–3]. These studies have focused on the design of the motor body or the efficiency of single motor running. But to the multi-motor drive system, the decoupling control, especially the dynamic decoupling control, is a valuable research direction in these applications.

Currently, the AC multi-motor drive system is the most popular in this field, which is a multi-input multi-output (MIMO), strong-coupling and nonlinear system. Under the influence of load variation and the interference factor, its structure characteristics or parameters are easily changed. So it is hard to obtain its accurate mathematical model. On the other hand, industrial production needs the multi-motor drive control to decouple the speed and the tension, which actually increases the control difficulty. This problem has become an important research topic of the electric drive control technology.

Received 2 June 2012; revised 29 January 2013.

†Corresponding author. E-mail: hzhang@ujs.edu.cn; Tel.: +86 511–88791960.

This work was supported by the National Natural Science Foundation of China (Nos.51007031, 51277194 and 61273154), the Specialized Research Fund for the Doctoral Program of Higher Education of China (No.20123227110012), the Natural Science Foundation of Jiangsu Province (No. BK2012711), the Priority Academic Program Development of Jiangsu Higher Education Institutions, and the Fund Program of Jiangsu University for Excellent Youth Teachers.

Common decoupling control methods mainly include: improved control algorithm based on the traditional PID control, cross-coupling control, feedforward control, optimal control, sliding mode control, fuzzy control[4–8]. More or less, these methods have improved decoupling effect. It should be specially noted that most of the existing control algorithms have strong dependence on the model of multi-motor system. However, when multi-motor system works in the different conditions and environments, its model and parameters will have a greater change. Thus, it is still difficult to ensure that the controlled system keeps optimal operation in the whole work process.

Recently, the neural network inverse theory was proposed[9–11]. This theory does not require an accurate model of the controlled system, and makes significant progress in decoupling research. The key of this theory is to build a pseudo-linear composite system, by using neural network to approximate the inverse system of the original system. Correspondingly, the control methods employed in the linear systems can be transplanted to the pseudo-linear composite system.

It is worth noticing that there exist some approximation errors when the neural network approximates inverse system, which will lead to steady-state errors in the results. Hence, it is necessary to design a kind of effective closed-loop controllers to compensate for the steady-state errors.

PID controller may be a choice as a closed-loop controller due to its advantages such as simple structure and easy to implement. However, given the complexity and time-varying of the controlled system, it is difficult to achieve the ideal starting and tracking effect by using PID controller whose parameters are kept constant. By contrast, an intelligent fuzzy self-tuning controller exhibits its unique superiority, which can on-line adjust the control parameters on the basis of the steady-error and the change rate of the steady-error. Fuzzy self-tuning control based on fuzzy linguistic variables, fuzzy set theory and fuzzy reasoning[12–15] which can improve overshoot residual defect. But it is prone to misoperation when the system fails.

In this paper, a new control strategy is proposed, in order to decouple the speed and tension of the three-motor drive system. The proposed strategy will combine fuzzy self-tuning control with back-propagation (BP) neural network generalized inverse (NNGI). On the one hand, NNGI achives the decoupling control of the MIMO system, which is not affected by parameter variation, reduced the dependence of the system model, and offers good nonlinear approximation ability. On the other hand, fuzzy self-tuning controller can on-line adjust the PID parameters and obviously improve the starting characteristics of the system，increase response speed and decrease system oscillation, which possess both the good steady-state precision, dynamic characteristics and strong robustness. The simulated results will be given for verification.

2 Mathematical model

Fig.1 shows the physical model of the three-AC-induction-motor drive system. It is laboratory-developed experimental platform to simulate the drives of the electric vehicle, rail transport, as well as rolling field. The system includes three 3-phase induction motors, SIENENS inverters, industrial control computer, PLC, tension sensor and photoelectric encoder. The control target is main motor speed and the tensions under the floating roller. The motor 1 is the main motor and other two motors are the subject ones. Every motor and its inverter can be regarded as a modular cell. The belt-pulley is installed on the motor shaft, and motors are combined by transmission belt on the belt-pulley. When the motors run, the rotation of their rotors pulls the belt to operate coordinately.

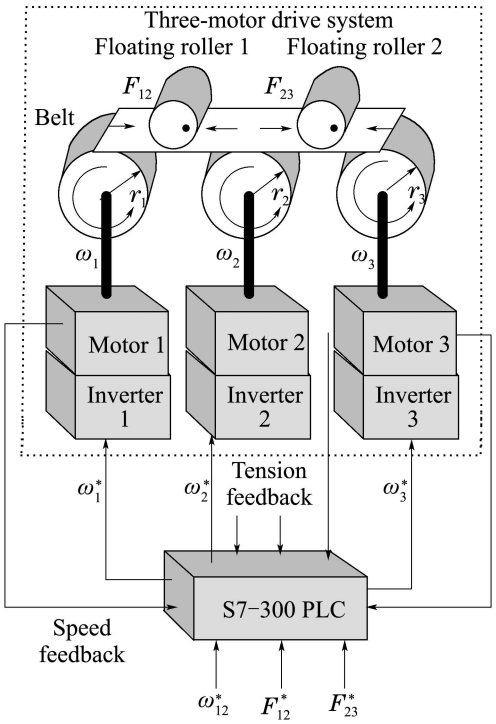

Fig. 1 Three motor drive system physical model

The tensions F_{12}, F_{22} of the belt are important parameters of the three-motor drive system's daily operation, which as variables must be maintained at some desired values when the motor's speed changes.

According to Hooke law and by considering the amount of forward slip, the tensions between the two adjacent motors can be expressed as

$$\begin{cases} \dot{F}_{12} = \dfrac{K_1}{T_1}\left(\dfrac{1}{n_{\mathrm{p1}}} r_1 k_1 \omega_{\mathrm{r1}} - \dfrac{1}{n_{\mathrm{p2}}} r_2 k_2 \omega_{\mathrm{r2}}\right) - \dfrac{F_{12}}{T_1}, \\ \dot{F}_{23} = \dfrac{K_2}{T_2}\left(\dfrac{1}{n_{\mathrm{p2}}} r_2 k_2 \omega_{\mathrm{r2}} - \dfrac{1}{n_{\mathrm{p3}}} r_3 k_3 \omega_{\mathrm{r3}}\right) - \dfrac{F_{23}}{T_2}, \end{cases} \tag{1}$$

where $K_1 = E/V_1$, $K_2 = E/V_2$ are the transfer coefficients; $T_1 = L_1/(AV_1)$, $T_2 = L_2/(AV_2)$ are the time constants of tension variation; $r_i, k_i, \omega_{\mathrm{r}i}$ are respectively the radius of No.i belt-pulley, the No.i speed ratio and the electric angular speed of No.i motor ($i = 1, 2, 3$); n_{pi} is the pole-pairs number of No.i motor ($i = 1, 2, 3$); A is the sectional area of the belt; E is Young's Modulus of the belt; L_1, L_2 are the distances between the two adjacent motors' racks; V_1, V_2 are the expected line speed.

When the system operates in field-oriented control mode, the mathematical model can be described as

$$\begin{cases}\dot{\omega}_{\rm r1}=\dfrac{n_{\rm p1}}{J_1}[(\omega_1-\omega_{\rm r1})\dfrac{n_{\rm p1}T_{\rm r1}}{L_{\rm r1}}\psi_{\rm r1}^2-\\ \qquad (T_{\rm L1}+r_1F_{12})],\\ \dot{\psi}_{\rm r1}=\dfrac{-1}{T_{\rm r1}}\psi_{\rm r1}+\dfrac{L_{\rm m1}}{T_{\rm r1}}i_{\rm sd1},\\ \dot{\omega}_{\rm r2}=\dfrac{n_{\rm p2}}{J_2}[(\omega_2-\omega_{\rm r2})\dfrac{n_{\rm p2}T_{\rm r2}}{L_{\rm r2}}\psi_{\rm r2}^2-\\ \qquad (T_{\rm L2}-r_2F_{12}+r_2F_{23})],\\ \dot{\psi}_{\rm r2}=\dfrac{-1}{T_{\rm r2}}\psi_{\rm r2}+\dfrac{L_{\rm m2}}{T_{\rm r2}}i_{\rm sd2},\\ \dot{\omega}_{\rm r3}=\dfrac{n_{\rm p3}}{J_3}[(\omega_3-\omega_{\rm r3})\dfrac{n_{\rm p3}T_{\rm r3}}{L_{\rm r3}}\psi_{\rm r3}^2-\\ \qquad (T_{\rm L3}-r_3F_{23})],\\ \dot{\psi}_{\rm r3}=\dfrac{-1}{T_{\rm r3}}\psi_{\rm r3}+\dfrac{L_{\rm m3}}{T_{\rm r3}}i_{\rm sd3},\\ \dot{F}_{12}=\dot{F}_{21}=\dfrac{K_1}{T_1}(\dfrac{1}{n_{\rm p1}}r_1k_1\omega_{\rm r1}-\\ \qquad \dfrac{1}{n_{\rm p2}}r_2k_2\omega_{\rm r2})-\dfrac{F_{12}}{T_1},\\ \dot{F}_{23}=\dfrac{K_2}{T_2}(\dfrac{1}{n_{\rm p2}}r_2k_2\omega_{\rm r2}-\dfrac{1}{n_{\rm p3}}r_3k_3\omega_{\rm r3})-\dfrac{F_{23}}{T_2},\end{cases}\tag{2}$$

where $J_{\rm i}$ is rotor inertia; $T_{{\rm r}i}$ is electromagnetic time constant; $T_{{\rm L}i}$ is load torque; $\psi_{{\rm r}i}$ is rotor flux; $L_{{\rm r}i}$ is rotor self-inductance; $i_{{\rm sd}i}$ is d-axis stator current; $\omega_{\rm i}$ is the synchronous angular speed of stator's frequency($i=1,2,3$).

3 Fuzzy self-tuning control based on generalized inverse system

3.1 Generalized inverse system

As an MIMO nonlinear system which has q dimension input vector $u=(u_1,u_2,\cdots,u_q)^{\rm T}\in\mathbb{R}^q$, q dimension output vector $y=(y_1,y_2,\cdots,y_q)^{\rm T}\in\mathbb{R}^q$, the differential equation can be expressed as

$$F(y^{(\varepsilon){\rm T}},Y,u^{(\sigma){\rm T}},U)=0,\tag{3}$$

where

$\varepsilon=(\varepsilon_1,\cdots,\varepsilon_q)^{\rm T}$, $\sigma=(\sigma_1,\cdots,\sigma_q)^{\rm T}$,

$y^{(\varepsilon)}=(y_1^{(\varepsilon_1)},\cdots,y_q^{(\varepsilon_q)})$, $u^{(\sigma)}=(u_1^{(\sigma_1)},\cdots,u_q^{(\sigma_q)})$,

$Y=(y_1^{(\varepsilon_1-1)},\cdots,y_1,\cdots,y_q^{(\varepsilon_q-1)},\cdots,y_q)^{\rm T}$,

$U=(u_1^{(\sigma_1-1)},\cdots,u_1,\cdots,u_q^{(\sigma_q-1)},\cdots,u_q)^{\rm T}$,

ε_j and σ_j are the highest derivative order of input u_j and output y_j.

When the relative-order of the system $\alpha=(\alpha_1,\alpha_2,\cdots,\alpha_q)^{\rm T}$ is existent, $\sum\limits_{j=1}^{q}\alpha_j=n$ in which (n is the order of the system), the state equation of the system can be transformed into differential equation. Besides, when the relative-order is equal to the original-order, the generalized inverse of the system can be directly obtained as

$$u=\bar{\varphi}(\bar{Y},\bar{\nu}),\tag{4}$$

where

$$\begin{aligned}\bar{Y}&=(y_1,y_1^{(1)},\cdots,y_1^{(\alpha_1-1)},\cdots,y_q,y_q^{(1)},\\ &\quad\cdots,y_q^{(\alpha_q-1)})^{\rm T},\\ \bar{\nu}&=(\bar{\nu}_1,\bar{\nu}_2,\cdots,\bar{\nu}_q)^{\rm T},\\ \bar{\nu_j}&=a_{j0}y_j+a_{j1}y_j^{(1)}+\cdots+\\ &\quad a_{j(\alpha_j-1)}y_j^{(\alpha_j-1)}+a_{j\alpha_j}y_j^{(\alpha_j)}.\end{aligned}$$

3.2 The structure of fuzzy self-tuning control system

Fuzzy self-tuning controller is a kind of intelligent controller, which uses fuzzy control rules to modify control parameters on-line. It primarily consists of fuzzy inference system and traditional PID controller. The fuzzy inference system regards the current error e and the change rate ec of error as its inputs, and then applies fuzzy reasoning method to adjust parameters $K_{\rm p}$, $K_{\rm i}$, $K_{\rm d}$ on-line, which can meet the requirement for PID parameters self-tuning at any time. The principle diagram of a fuzzy self-tuning control system is given in Fig.2.

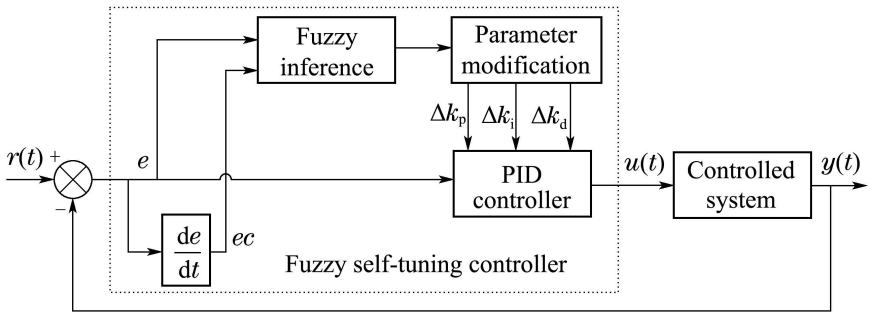

Fig. 2 Fuzzy self-tuning control system principle diagram

From the above illustration, it can be clearly found that the cores of the fuzzy self-tuning control system are the fuzzy inference system and PID controller. The traditional PID controller is a kind of linear controller. It gets error $e(t)$ according to the difference between the given value $r(t)$ and the actual output value $y(t)$, and then regulates the controlled object by the control value $u(t)$ which is the linear combination of $e(t)'$ s proportion, integral and derivative.

The structure diagram of PID controller is shown in Fig.3. The relationship between the input and the output can be expressed as

$$u(t)=K_{\rm p}e(t)+K_{\rm i}\int_0^t e(\tau){\rm d}\tau+K_{\rm d}\frac{{\rm d}e(t)}{{\rm d}t},\tag{5}$$

where $K_{\rm p}$ is the proportional gain; $K_{\rm i}$ is the integral gain; $K_{\rm d}$ is the derivative gain.

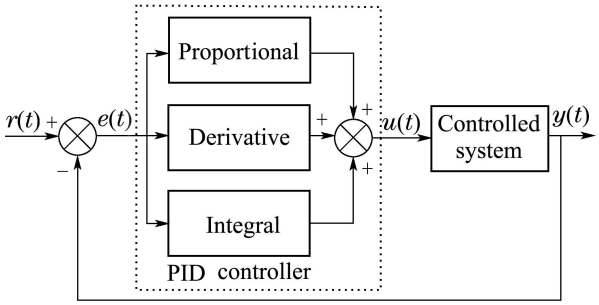

Fig. 3 PID controller structure diagram

3.3 Fuzzy factor and ambiguity-resolving factor

Each input variable of the fuzzy self-tuning controller has been defined in a corresponding domain, however, the actual system's error e and the change rate ec of the error may not belong to this range. Therefore the two input variables need to be multiplied by smaller fuzzy factors k_{e} and k_{ec}, respectively, make sure to be in this range. Meanwhile, the output variables need to be multiplied by ambiguity-resolving factors f_{p}, f_{i}, and f_{d}, which are established based on experience respectively.

The ultimate gain coefficients can be expressed as follows:

$$K_{\mathrm{p}} = K_{\mathrm{p}}^0 + K_{\mathrm{p}}^* \times f_{\mathrm{p}} = K_{\mathrm{p}}^0 + \Delta K_{\mathrm{p}}, \tag{6}$$

$$K_{\mathrm{i}} = K_{\mathrm{i}}^0 + K_{\mathrm{i}}^* \times f_{\mathrm{i}} \ = K_{\mathrm{i}}^0 + \Delta K_{\mathrm{i}}, \tag{7}$$

$$K_{\mathrm{d}} = K_{\mathrm{d}}^0 + K_{\mathrm{d}}^* \times f_{\mathrm{d}} = K_{\mathrm{d}}^0 + \Delta K_{\mathrm{d}}, \tag{8}$$

where K_{p}^0, K_{i}^0 and K_{d}^0 are the initial values of the gain coefficients; K_{p}^*, K_{i}^* and K_{d}^* are the fuzzy calculated output values; ΔK_{p}, ΔK_{i} and ΔK_{d} are the variations of the gain coefficients.

4 Specific design of the control system

4.1 The solution to generalized inverse system

When the inverters work in vector mode, the rotor flux is considered to be unchanged. So, the mathematic model of the system can be rewritten as

$$\dot{x} = f(x,u) = \begin{bmatrix} \frac{n_{\mathrm{p1}}}{J_1}[(\omega_1 - \omega_{\mathrm{r1}})\frac{n_{\mathrm{p1}}T_{\mathrm{r1}}}{L_{\mathrm{r1}}}\psi_{\mathrm{r1}}^2 - (T_{\mathrm{L1}} + r_1F_{12})] \\ \frac{n_{\mathrm{p2}}}{J_2}[(\omega_2 - \omega_{\mathrm{r2}})\frac{n_{\mathrm{p2}}T_{\mathrm{r2}}}{L_{\mathrm{r2}}}\psi_{\mathrm{r2}}^2 - (T_{\mathrm{L2}} - r_2F_{12} + r_2F_{23})] \\ \frac{n_{\mathrm{p3}}}{J_3}[(\omega_3 - \omega_{\mathrm{r3}})\frac{n_{\mathrm{p3}}T_{\mathrm{r3}}}{L_{\mathrm{r3}}}\psi_{\mathrm{r3}}^2 - (T_{\mathrm{L3}} - r_3F_{23})] \\ \frac{K_1}{T_1}(\frac{1}{n_{\mathrm{p1}}}r_1k_1\omega_{\mathrm{r1}} - \frac{1}{n_{\mathrm{p2}}}r_2k_2\omega_{\mathrm{r2}}) - \frac{F_{12}}{T_1} \\ \frac{K_2}{T_2}(\frac{1}{n_{\mathrm{p2}}}r_2k_2\omega_{\mathrm{r2}} - \frac{1}{n_{\mathrm{p3}}}r_3k_3\omega_{\mathrm{r3}}) - \frac{F_{23}}{T_2} \end{bmatrix}. \tag{9}$$

State variable is

$$x = [x_1 \ x_2 \ x_3 \ x_4 \ x_5]^{\mathrm{T}} = [\omega_{\mathrm{r1}} \ \omega_{\mathrm{r2}} \ \omega_{\mathrm{r3}} \ F_{12} \ F_{23}]^{\mathrm{T}}.$$

Control variable is

$$u = [u_1 \ u_2 \ u_3]^{\mathrm{T}} = [\omega_1 \ \omega_2 \ \omega_3]^{\mathrm{T}}.$$

Output variable is

$$y = [y_1 \ y_2 \ y_3]^{\mathrm{T}} = [\omega_{\mathrm{r1}} \ F_{12} \ F_{23}]^{\mathrm{T}}.$$

The corresponding Jacobi matrix is

$$J(x,u) = \begin{bmatrix} \frac{\partial y_1^{(1)}}{\partial u_1} & \frac{\partial y_1^{(1)}}{\partial u_2} & \frac{\partial y_1^{(1)}}{\partial u_3} \\ \frac{\partial y_2^{(2)}}{\partial u_1} & \frac{\partial y_2^{(2)}}{\partial u_2} & \frac{\partial y_2^{(2)}}{\partial u_3} \\ \frac{\partial y_3^{(2)}}{\partial u_1} & \frac{\partial y_3^{(2)}}{\partial u_2} & \frac{\partial y_3^{(2)}}{\partial u_3} \end{bmatrix} = \begin{bmatrix} \frac{n_{\mathrm{p1}}^2T_{\mathrm{r1}}\psi_{\mathrm{r1}}^2}{J_1L_{\mathrm{r1}}} & 0 & 0 \\ \frac{K_1r_1k_1n_{\mathrm{p1}}T_{\mathrm{r1}}\psi_{\mathrm{r1}}^2}{T_1J_1L_{\mathrm{r1}}} & -\frac{K_1r_2k_2n_{\mathrm{p2}}T_{\mathrm{r2}}\psi_{\mathrm{r2}}^2}{T_1J_2L_{\mathrm{r2}}} & 0 \\ 0 & \frac{K_2r_2k_2n_{\mathrm{p2}}T_{\mathrm{r2}}\psi_{\mathrm{r2}}^2}{T_2J_2L_{\mathrm{r2}}} & -\frac{K_2r_3k_3n_{\mathrm{p3}}T_{\mathrm{r3}}\psi_{\mathrm{r3}}^2}{T_2J_3L_{\mathrm{r3}}} \end{bmatrix},$$

$$\mathrm{Det}(J(x,u)) = \frac{K_1K_2r_2r_3k_2k_3n_{\mathrm{p1}}^2n_{\mathrm{p2}}n_{\mathrm{p3}}T_{\mathrm{r1}}T_{\mathrm{r2}}T_{\mathrm{r3}}\psi_{\mathrm{r1}}^2\psi_{\mathrm{r2}}^2\psi_{\mathrm{r3}}^2}{T_1T_2J_1J_2J_3L_{\mathrm{r1}}L_{\mathrm{r2}}L_{\mathrm{r3}}}. \tag{10}$$

When $\psi_{\mathrm{r1}} \neq 0$, $\psi_{\mathrm{r2}} \neq 0$, $\psi_{\mathrm{r3}} \neq 0$, $J(x,u)$ is non-singular. The relative-order of system is $\alpha = (1,2,2)$, $\alpha_1+\alpha_2+\alpha_3 = 1+2+2 = 5 = n$ (order of system), so the generalized inverse of system is existent. Original-order of system $n_{\mathrm{e}} = n_{e1} + n_{e2} + n_{e3} = 1+2+2 = 5 = \alpha =$ relative-order, so the generalized inverse of system is

$$u = \bar{\varphi}(\{y_1, y_2, y_2^{(1)}, y_3, y_3^{(1)}\}, \bar{\nu}), \tag{11}$$

where

$$\begin{aligned} &\bar{\nu} = (\bar{\nu_1}, \bar{\nu_2}, \bar{\nu_3})^{\mathrm{T}}, \\ &\bar{\nu_1} = a_{10}y_1 + a_{11}y_1^{(1)}, \\ &\bar{\nu_2} = a_{20}y_2 + a_{21}y_2^{(1)} + a_{22}y_2^{(2)}, \\ &\bar{\nu_3} = a_{30}y_3 + a_{31}y_3^{(1)} + a_{32}y_3^{(2)}. \end{aligned}$$

4.2 The construction of pseudo-linear composite system

Connected by the generalized inverse system serially, the original system can be decoupled and then simplified into a first-order speed subsystem and two best second-order tension subsystems. Accordingly, the pseudo-linear composite system can be obtained, as shown in Fig.4. NNGI open-loop control diagram is shown in Fig.5.

The transfer function is

$$G(S) = \mathrm{diag}\{G_{11}, G_{22}, G_{33}\} = \mathrm{diag}\{\frac{1}{s+1}, \frac{1}{s^2+1.414s+1}, \frac{1}{s^2+1.414s+1}\}, \tag{12}$$

where $(s+1)^{-1}$ is speed subsystem, $(s^2+1.414s+1)^{-1}$ is tension subsystem.

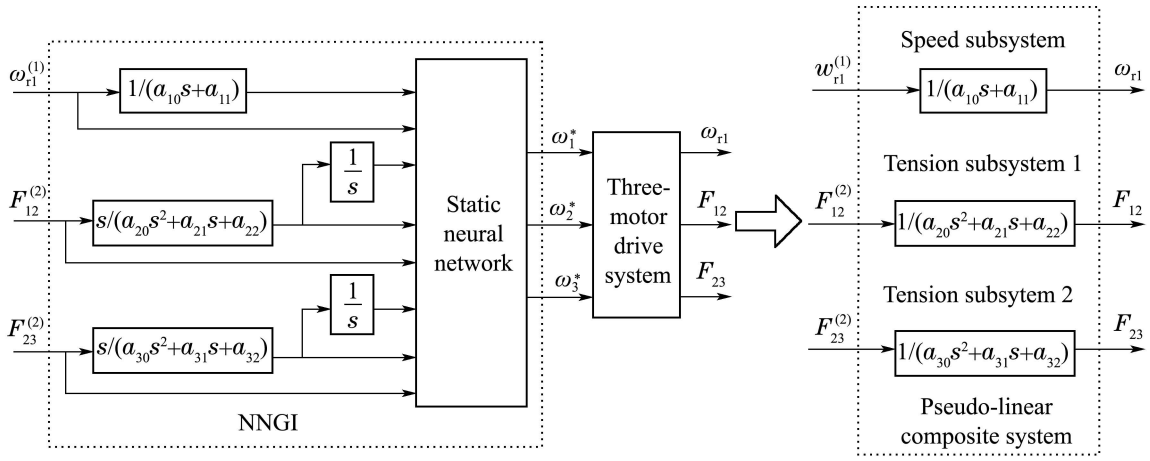

Fig. 4 Pseudo-linear composite system equivalent chart

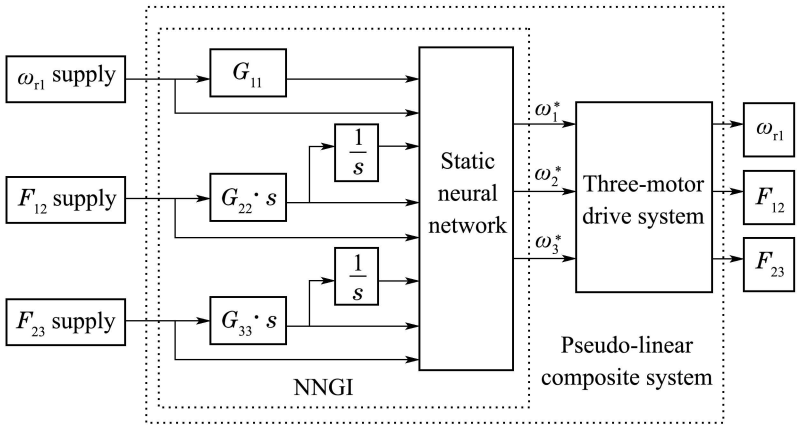

Fig. 5 NNGI open-loop control diagram

4.3 The design of fuzzy self-tuning controller

The form of two inputs and three outputs is determined for the fuzzy self-tuning controller. Input variables include e and ec; and output variables include the fuzzy calculated output values: $K_{\rm p}^*, K_{\rm i}^*$ and $K_{\rm d}^*$. The fuzzy subset of input and output variables is {NB, NM, NS, ZO, PS, PM, PB}, in which the elements represent 'negative', 'big', 'negative middle', 'negative small', 'zero', 'positive small', 'positive middle', 'positive big', the corresponding quantization levels are represented by transverse coordinate scale as shown in Figs.7−9. The domain of e is $[-3,3]$, ec is $[-3,3]$, $K_{\rm d}^*$ is $[-3,3]$, $K_{\rm p}^*$ is $[-0.3,0.3]$, and $K_{\rm i}^*$ is $[-0.06,0.06]$. The structure of fuzzy self-tuning controller is shown in Fig.6.

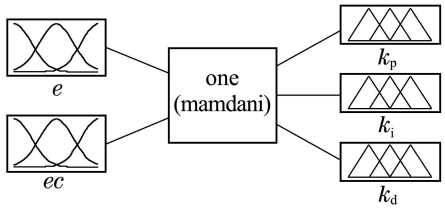

Fig. 6 Fuzzy self-tuning controller structure

As PID regulation, fuzzy factors and ambiguity-resolving factors are determined according to practical experience. We first adjust the fuzzy factor $k_{\rm e}$, $k_{\rm ec}$ before adjusting the solution fuzzy factor $f_{\rm p}$, $f_{\rm i}$, $f_{\rm d}$.

Step 1 Increases $k_{\rm e}$ can reduce the rise time of the system, to speed up the adjustment speed, but $k_{\rm e}$ can not be too large, otherwise it will lead to a larger overshoot, the system produces shock. Increasing the $k_{\rm ec}$ can reduce system overshoot, but slows down the system response speed, $k_{\rm ec}$ too large will also increase the regulation time.

Step 2 The solution fuzzy factor is the proportional gain of the fuzzy control output, and the specific adjustment is as follows: 1) Increase the $f_{\rm p}$ will speed up the system response speed, but excessive $f_{\rm p}$ will cause overshoot. 2) Increase the $f_{\rm i}$ will reduce the system steady state time, but excessive $f_{\rm i}$ also cause overshoot. 3) Increase the $f_{\rm d}$ will be able to suppress the overshoot of the system, increasing the adjustment time.

In the experiment, the PID parameters are on-line adjusted on the basis of the steady-error and the change rate of the steady-error. Therefore, the parameters in the first fuzzy self-tuning controller:

$$K_{\rm p}^0 = 0.8,\ K_{\rm i}^0 = 0.5,\ K_{\rm d}^0 = 0,\ k_{\rm e} = 0.042,$$
$$k_{\rm ec} = 0.05,\ f_{\rm p} = 0.1,\ f_{\rm i} = 0.1,\ f_{\rm d} = 0.$$

In the second fuzzy self-tuning controller:

$$K_{\rm p}^0 = 0.4,\ K_{\rm i}^0 = 0.35,\ K_{\rm d}^0 = 0,\ k_{\rm e} = 1.5,$$
$$k_{\rm ec} = 1.2,\ f_{\rm p} = 0.1,\ f_{\rm i} = 1,\ f_{\rm d} = 0.$$

In the third fuzzy self-tuning controller:

$$K_{\rm p}^0 = 0.4,\ K_{\rm i}^0 = 0.35,\ K_{\rm d}^0 = 0,\ k_{\rm e} = 0.5,$$
$$k_{\rm ec} = 0.4,\ f_{\rm p} = 0.1,\ f_{\rm i} = 1,\ f_{\rm d} = 0.$$

To the all input and output variables, the membership functions for the elements NB and PB adopt 'zmf' ,'smf' , respectively. For the other elements, 'trimf' is chosen as the membership function. The membership functions of the inputs and outputs are shown in Fig.7 to Fig.9.

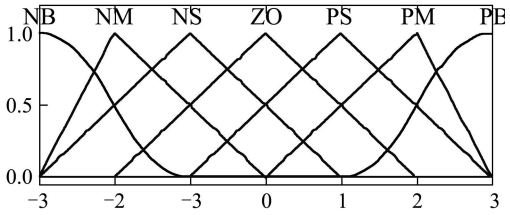

Fig. 7 The membership function of $e, ec, K_{\mathrm{d}}^{*}$

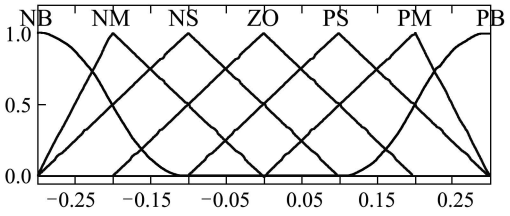

Fig. 8 The membership function of K_{p}^{*}

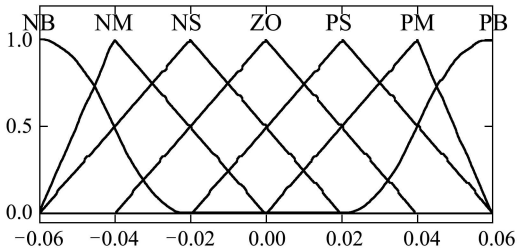

Fig. 9 The membership function of K_{i}^{*}

On the premise of PID parameter tuning principles, the fuzzy control rules of K_{p}^{*}, K_{i}^{*}, and K_{d}^{*} are established based on experience. The fuzzy rule-base is shown in Table 1, in which there are totally 49 control rules:

If (e is NB) and (ec is NB),
then (K_{p}^{*} is PB)(K_{i}^{*} is NB)(K_{d}^{*} is PS),
⋮
If (e is PB) and (ec is PB),
then (K_{p}^{*} is NB)(K_{i}^{*} is PB)(K_{d}^{*} is PB).

On the basis of NNGI open-loop control system as the Fig.5 shows, fuzzy self-tuning NNGI control system is constructed by adding the fuzzy self-tuning controllers, which is shown in Fig.10.

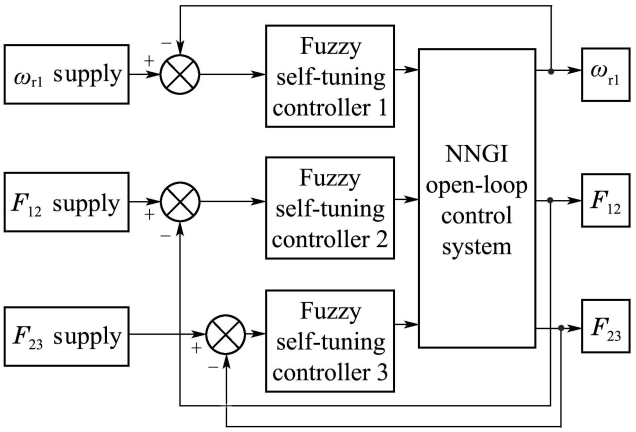

Fig. 10 Fuzzy self-tuning NNGI control diagram

Table 1 The fuzzy rule-base for $K_{\mathrm{p}}^{*}, K_{\mathrm{i}}^{*}, K_{\mathrm{d}}^{*}$

e	ec						
	NB	NM	NS	ZO	PS	PM	PB
NB	PB/NB/PS	PB/NB/NS	PM/NM/PB	PM/NM/NB	PS/NS/NB	ZO/ZO/NM	ZO/ZO/PS
NM	PB/NB/PS	PB/NB/NS	PM/NM/PB	PS/NS/NM	PS/NS/NM	ZO/ZO/NS	NS/ZO/ZO
NS	PM/NB/ZO	PM/NM/NS	PM/NS/NM	PS/NS/NM	ZO/ZO/NS	NS/PM/NS	NS/PM/ZO
ZO	PM/NM/ZO	PM/NM/NS	PS/NS/NS	ZO/ZO/NS	NS/PS/NS	NM/PM/NS	NM/PM/ZO
PS	PS/NM/ZO	PS/NS/ZO	ZO/ZO/ZO	NS/PS/ZO	NS/PS/ZO	NM/PM/ZO	NM/PB/ZO
PM	PS/ZO/PB	ZO/ZO/NS	NS/PS/PS	NM/PS/PS	NM/PM/PS	NM/PB/PS	NB/PB/PB
PB	ZO/ZO/PB	ZO/ZO/PM	NM/PS/PM	NM/PM/PM	NM/PM/PS	NB/PB/PS	NB/PB/PB

5 Simulations

5.1 Modeling

According to (2), the simulation model of the three-motor drive system is built up in the software environment of MATLAB/Simulink. Three-motor drive system parameters are set as follows: The numbers of pole pairs are set to $n_{\mathrm{p1}} = 2,\ n_{\mathrm{p2}} = 2,\ n_{\mathrm{p3}} = 2$. The moment inertia $J_1 = 0.6\,\mathrm{kg}\cdot\mathrm{m}^2,\ J_2 = 0.5\,\mathrm{kg}\cdot\mathrm{m}^2,\ J_3 = 0.4\,\mathrm{kg}\cdot\mathrm{m}^2$. Electromagnetic time constant $T_{\mathrm{r1}} = 0.5\,\Omega,\ T_{\mathrm{r2}} = 0.5\,\Omega,\ T_{\mathrm{r3}} = 0.5\,\Omega$. The rotor inductance $L_{\mathrm{r1}} = 0.2\,\mathrm{H},\ L_{\mathrm{r2}} = 0.3\,\mathrm{H},\ L_{\mathrm{r3}} = 0.25\,\mathrm{H}$. The mutual inductance $L_{\mathrm{m1}} = 0.1\,\mathrm{H},\ L_{\mathrm{m2}} = 0.2\,\mathrm{H},\ L_{\mathrm{m3}} = 0.15\,\mathrm{H}$. Pulley radius $r_1 = 0.1\,\mathrm{m},\ r_2 = 0.09\,\mathrm{m},\ r_3 = 0.15\,\mathrm{m}$. The speed radio $k_1 = k_2 = k_3 = 1/15$. In the Eq. (11), the parameters are as follows: $a_{10} = 1,\ a_{11} = 1$; $a_{20} = 1,\ a_{21} = 1.414,\ a_{22} = 1$; $a_{30} = 1,\ a_{31} = 1.414,\ a_{32} = 1$.

At first, the three-motor drive system is motivated by using the given random square waves of the speed and tensions, so a set of sampled data can be obtained, as shown in Fig.11. Then this set of data is used to train the BP neural network, so as to get the NNGI system. It must be noted that the input data and output data of the neural network should be normalized and anti-normalized, respectively. Secondly, the generated neural network is connected before the original system in series to constitute pseudo-linear composite system and NNGI open-loop control system. Lastly, the fuzzy self-tuning controllers (related settings as mentioned above) are added as the closed-loop controllers to form the fuzzy self-tuning NNGI control system.

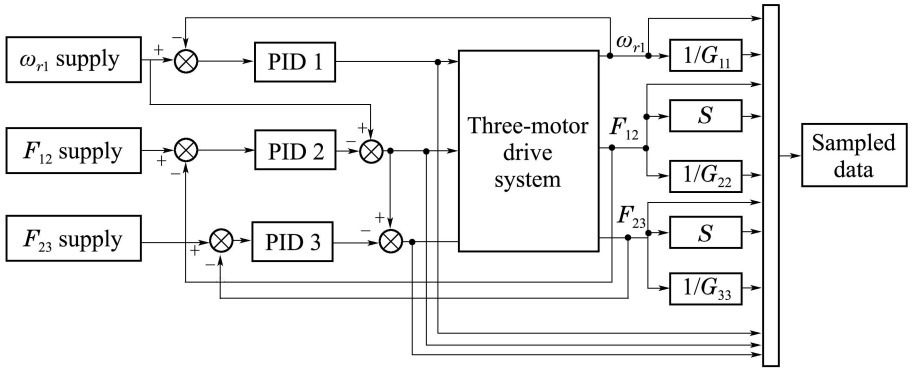

Fig. 11 System excitation simulation structure

5.2 Results

In order to test the decoupling effect of the control system, $\omega_{\rm r1}$ is set to increase and then suddenly decrease in the range of 200∼300 r/min. Meanwhile, F_{12} and F_{23} are set to constant 30 kg and 35 kg, respectively. The simulated step response waveforms with PID control, NNGI open-loop control and fuzzy adaptive NNGI control are compared in Figs.12−14.

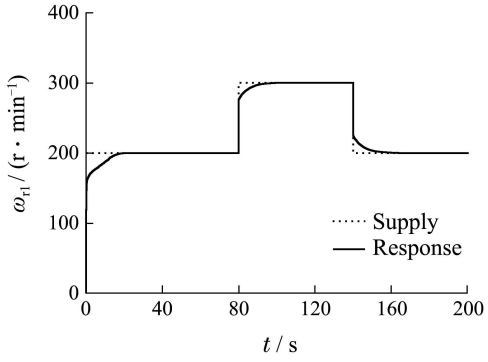

(a) $\omega_{\rm r1}$

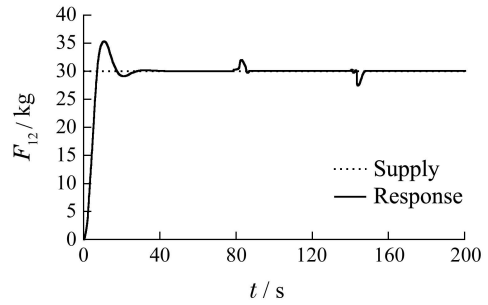

(b) F_{12}

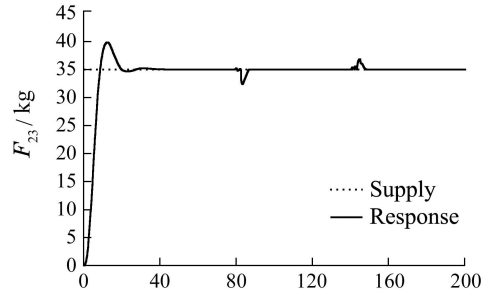

(c) F_{23}

Fig. 12 Simulated step responses of PID control when $\omega_{\rm r1}$ suddenly changes

Fig.12 demonstrates that traditional PID control can not solve strong coupling problem when the speed $\omega_{\rm r1}$ suddenly increases or suddenly decreases, because the tensions F_{12} and F_{23} occur to fluctuate dramatically. In contrast, once NNGI open-loop control is adopted, the decoupling problem can be settled, but there exist some steady-state errors in system response, as shown in Fig.13.

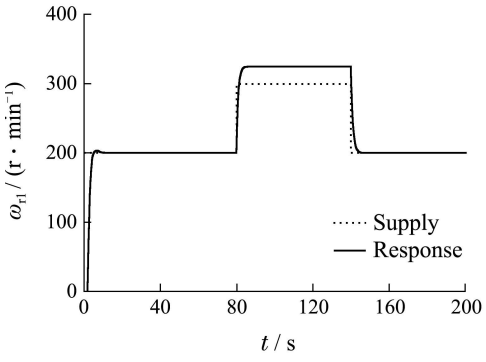

(a) $\omega_{\rm r1}$

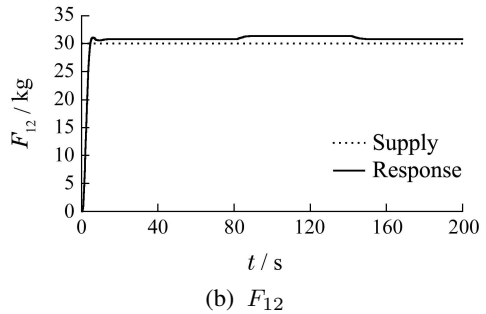

(b) F_{12}

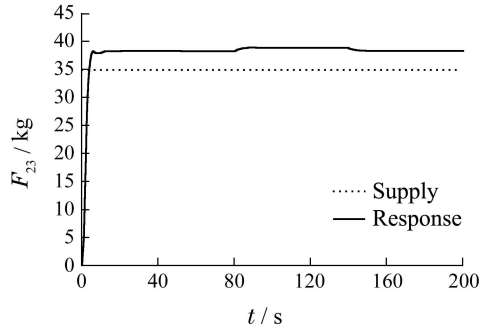

(c) F_{23}

Fig. 13 Simulated step responses of NNGI open-loop control when $\omega_{\rm r1}$ suddenly changes

To overcome this defect, fuzzy self-tuning controllers are added as the closed-loop controllers in Fig.14, so the

steady-state errors are completely eliminated. This illustrates that the proposed strategy can not only achieve the stability of the three-motor drive system, but also effectively solve strong coupling problems. Far more importantly, it obviously has excellent starting characteristics with rapid response speed, slight overshoot and short transient time, and has no system oscillation when the response reaches the steady state.

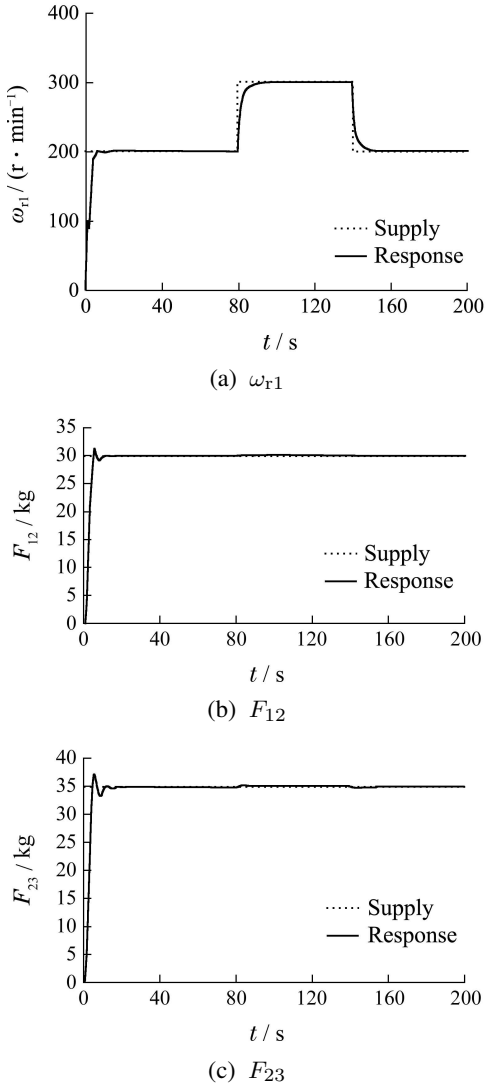

Fig. 14 Simulated step responses of fuzzy self-tuning NNGI control when ω_{r1} suddenly changes

Given the fact that any complex given signal can be composed of many sine waves with different frequencies and different amplitudes, two different conditions are set separately to check the tracking performance of the control system: 1) F_{12} and F_{23} are kept constant, while ω_{r1} is set to track the 200∼300 r/min sine wave with a cycle of 50 s, as shown in Fig.15. 2) ω_{r1} and F_{23} are maintained constant, while F_{12} is set to track the 29∼31 kg sine wave with a cycle of 50 s, as shown in Fig.16. Fig.15 manifests that the proposed control method offers superior tracking effect. Because of the existence of the fuzzy self-tuning controllers, there are no steady-state errors in the response, so the speed can tracks the square wave with no difference while remaining the tensions invariant. In Fig.16, when the given signal of F_{12} is sine wave, it also appears good tracking performance, especially high tracking accuracy and fast tracking speed.

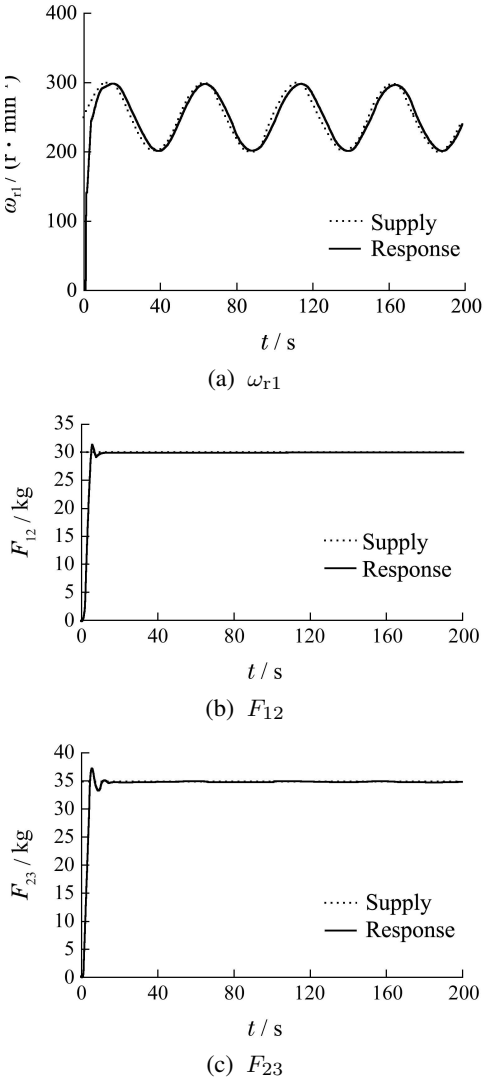

Fig. 15 Simulated tracking responses when ω_{r1} suddenly changes in the form of sine waves

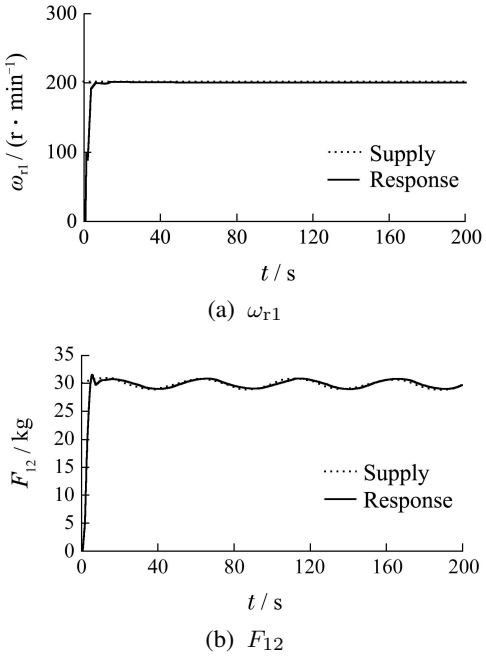

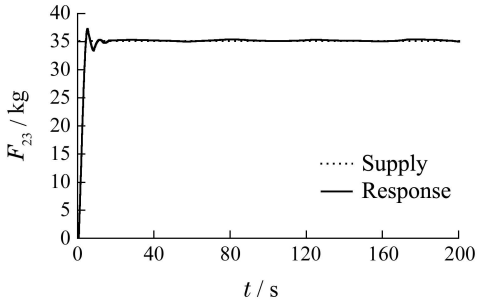

(c) F_{23}

Fig. 16 Simulated tracking responses when F_{12} suddenly changes in the form of sine waves

6 Conclusions

In this paper, a new control strategy has been proposed to decouple the speed and the tension of the three-motor drive system by combining NNGI with fuzzy self-tuning controller. This kind of intelligent controller can on-line adjust the control parameters on the basis of the steady-error and the change rate of the steady-error to achieve the desired control effect. The simulated results verify that the proposed strategy can validly attain decoupling the speed and the tension, in which process the three-motor drive system is transformed into several SISO linear subsystems with open-loop stability. Moreover, it has obviously superiority including rapid response speed, slight overshoot, short transient time and good tracking effect, which help to improve the starting characteristics of the system and decrease system oscillation. This new control strategy is particularly practical and effective for many industrial drive applications as economy advances.

References:

[1] CHAU K T, CHAN C C, LIU C H. Overview of permanent-magnet brushless drives for electric and hybrid electric vehicles [J]. *IEEE Transactions on Industrial Electronics*, 2008, 55(6): 2246 – 2257.

[2] LEVI E, JONES M, VUKOSAVIC S N, et al. Operating principles of a novel multiphase multimotor vector-controlled drive [J]. *IEEE Transactions on Energy Conversion*, 2004, 19(3): 508 – 517.

[3] PESSINA G, MORRA E. Reliability evaluation of a multi-motor drive system for daily newspaper printing plants [C] *//International Symposium on Power Electronics, Electrical Drives, Automation and Motion*. SPEEDAM: IEEE, 2006: 1408 – 1412.

[4] ZHAO D Z, LI C W, REN J. Speed synchronisation of multiple induction motors with adjacent cross-coupling control [J]. *IET Control Theory and Applications*, 2010, 4(1): 119 – 128.

[5] CHENG B, TESCH T R. Torque feedforward control technique for permanent-magnet synchronous motors [J]. *IEEE Transactions on Industrial Electronics*, 2010, 57(3): 969 – 974.

[6] YANG Y P, CHUANG D S. Optimal design and control of a wheel motor for electric passenger cars [J]. *IEEE Transactions on Magnetics*, 2007, 43(1): 51 – 61.

[7] ABJADI N R, SOLTANI J, MARKADEH J. Nonlinear sliding-mode control of a multi-motor web-winding system without tension sensor [J]. *IET Control Theory and Applications*, 2009, 3(4): 419 – 427.

[8] CHEN C. TSK-type self-organizing recurrent-neural-fuzzy control of linear microstepping motor drives [J]. *IEEE Transactions on Power Electronics*, 2010, 25(9): 2253 – 2265.

[9] DAI X, HE D, ZHANG T, et al. ANN generalised inversion for the linearisation and decoupling control of nonlinear systems [J]. *IEE Proceedings on Control Theory and Applications*, 2003, 150(3): 267 – 277.

[10] DAI X, HE D, ZHANG X, et al. MIMO system invertibility and decoupling control strategies based on ANN alpha th-order inversion [J]. *IEE Proceedings on Control Theory and Applications*, 2001, 148(2): 125 – 136.

[11] YU D, LIU F, LAI P, et al. Nonlinear dynamic compensation of sensors using inverse-model-based neural network [J]. *IEEE Transactions on Instrumentation and Measurement*, 2008, 57(10): 2364 – 2376.

[12] CHIU C. Mixed feedforward/feedback based adaptive fuzzy control for a class of MIMO nonlinear systems [J]. *IEEE Transactions on Fuzzy Systems*, 2006, 14(6): 716 – 727.

[13] CHEN B, LIU X, TONG S. Adaptive fuzzy output tracking control of MIMO nonlinear uncertain systems [J]. *IEEE Transactions on Fuzzy Systems*, 2007, 15(2): 287 – 300.

[14] LIU J, MARTIN G. *MATLAB Simulation of Advanced PID Control* [M]. Beijing: Publishing House of Electronics Industry, 2003.

[15] KUNG Y, TSAI M. FPGA-based speed control IC for PMSM drive with adaptive fuzzy control [J]. *IEEE Transactions on Power Electronics*, 2007, 22(6): 2476 – 2486.

作者简介:

张 浩 (1976–), 男, 讲师, 博士研究生, 目前研究方向为电机驱动、神经网络控制, E-mail: hzhang@ujs.edu.cn;

于 堃 (1986–), 男, 博士研究生, 目前研究方向为电机驱动、图像处理, E-mail: yukunemail@163.com;

刘国海 (1964–), 男, 教授, 博士生导师, 目前研究方向为电机驱动、智能控制, E-mail: ghliu@ujs.edu.cn;

胡德水 (1983–), 男, 硕士研究生, 目前研究方向为电机驱动, E-mail: hudeshui7547@163.com;

赵文祥 (1976–), 男, 副教授, 博士, 目前研究方向为电机设计、容错控制, E-mail: zwx@ujs.edu.cn.